Published in final edited form as:
Sci Signal. ; 6(261): ra9. doi:10.1126/scisignal.2003730.

Sterical hindrance promotes selectivity of the autophagy cargo receptor NDP52 for the danger receptor galectin-8 in anti-bacterial autophagy

Sai Li[1,*], **Michal P. Wandel**[2,*], **Fudong Li**[1], **Zhonghua Liu**[1], **Chao He**[1], **Jihui Wu**[1], **Yunyu Shi**[1,§], and **Felix Randow**[2,§]

[1]Hefei National Laboratory for Physical Sciences at Microscale and School of Life Sciences, University of Science and Technology of China, Hefei, Anhui, 230026, China

[2]MRC Laboratory of Molecular Biology, Division of Protein and Nucleic Acid Chemistry, Hills Road, Cambridge CB2 0QH, UK

Abstract

Autophagy, the process of lysosome-dependent degradation of cytosolic components, is a mechanism by which cells selectively engulf invading pathogens to protect themselves against infection. Galectin-8, a cytosolic lectin with specificity for β-galactosides, binds endosomal and lysosomal membranes that have been damaged, for example by pathogens, and selectively recruits the autophagy cargo receptor NDP52 to induce autophagy. Here, we solved the crystal structure of the NDP52–galectin-8 complex to show how NDP52 exclusively binds galectin-8 and, consequently, why other galectins do not restrict the growth of *Salmonella* in human cells.

Introduction

Macro-autophagy, a lysosome-dependent degradation pathway for cytosolic components, controls a multitude of cellular processes, such as the response to starvation, the degradation of protein aggregates, the elimination of damaged or superfluous organelles, and the defense against invading pathogens (1-3). In contrast to the indiscriminate engulfment of cytosol into autophagosomes during starvation, selective autophagy is mediated by specific 'eat-me' signals detected by specialized cargo receptors (4). Selective autophagy of bacteria is initiated by three receptors, NDP52, p62, and optineurin, which detect bacteria-associated poly-ubiquitylated proteins (5-7). NDP52 also senses galectin-8, which functions as a ubiquitin-independent 'eat-me' signal on vesicles damaged by cytosol-invading bacteria (8).

Galectins are cytosolic lectins, i.e. sugar-binding proteins, with specificity for β-galactoside-containing glycans (9, 10). In mammalian cells under homeostatic conditions, such glycans

§Correspondence should be addressed to Yunyu Shi (Tel: +86 551 3607464; Fax: +86 551 3601443; yyshi@ustc.edu.cn) or Felix Randow (Tel: +44 1223 252986; Fax: +44 1223 412178; randow@mrc-lmb.cam.ac.uk). .
*These authors contributed equally to this work.

Author contributions: SL protein purification, crystallization, mutagenesis, ITC measurements, structural analysis; MPW LUMIER assays and *Salmonella* infections; FL structure determination and analysis, ITC measurements; ZL and CH protein sample preparation, crystallographic studies and ITC experiments; JW data analysis. FR and YS designed the overall research and wrote the paper. All authors discussed the results and commented on the manuscript.

One-sentence summary A crystal structure of an autophagy receptor with a ligand reveals how *Salmonella* is specifically targeted for degradation.

Accession code. The structure coordinates and structure factors of $Gal8_{C\text{-}CRD}$ in complex with $NDP52_{368\text{-}381}$ have been deposited in the Protein Data Bank (PDB) under accession numbers 4GXL.

Competing interests: The authors declare that they have no competing interests.

Europe PMC Funders Author Manuscripts

are found exclusively in extracellular compartments including the lumen of vesicles. A breach in membrane integrity, which may be caused by vesicle-damaging pathogens, such as *Salmonella enterica* serovar Typhimurium (*S.* Typhimurium), *Listeria monocytogenes*, or *Shigella flexneri*, introduces glycans into the cytosol, which cells perceive as an acute danger signal (3). The human genome encodes about a dozen galectins, of which galectin-1, 3, 8, and 9 bind glycans on damaged endosomes or lysosomes in epithelial cells (8, 9, 11), thereby inducing autophagy, inflammatory signaling, and possibly other cellular responses (8, 11). Currently, the only known effector protein of galectin-sensed membrane damage is NDP52, an LC3C-binding autophagy receptor that restricts the proliferation of *S.* Typhimurium upon entry into the cytosol by targeting galectin-8–associated bacteria for autophagy (5, 8, 12). NDP52 contains a short peptide ($NDP52_{372\text{-}380}$) that binds the C-terminal carbohydrate recognition domain (CRD) of galectin-8 ($Gal8_{C\text{-}CRD}$) with high selectivity, which explains why galectin-8, but not other membrane damage-sensing galectins, can induce NDP52-mediated autophagy of vesicles damaged by the presence of *S.* Typhimurium and thus restrict the proliferation of this pathogen inside human cells (8).

Here, we solved the crystal structure of NDP52 bound to $Gal8_{C\text{-}CRD}$ to show how galectin-8, uniquely amongst galectins, binds NDP52. $NDP52_{371\text{-}381}$ formed a hook-like structure that strategically positions several side chains for mainly hydrophobic contacts with galectin-8. Interference with the hook formation, as well as mutations in contact residues, abrogated binding between NDP52 and $Gal8_{C\text{-}CRD}$ and impeded autophagy of *S.* Typhimurium. Binding of NDP52 to other galectins was prevented primarily by sterical hindrance in the CRDs of galectins that did not bind, rather than the lack of conserved contact residues in these CRDs, thus explaining the selectivity of NDP52 for galectin-8..

Results

Structural basis for the binding of the danger receptor galectin-8 to the autophagy adaptor NDP52

To characterize how galectins recruit effector proteins and to understand how specificity between NDP52 and galectin-8 is achieved, we solved the crystal structure of $Gal8_{C\text{-}CRD}$ (residues 228-359) in complex with $NDP52_{368\text{-}381}$ at 2.0 ångströms (Å) resolution (Table 1). Similar to other galectins (13-15), $Gal8_{C\text{-}CRD}$ adopted a bent β-sandwich structure formed by two antiparallel β-sheets of six and five strands, which comprise the concave and convex surface, respectively (Fig. 1A, fig. S1). Galectins bind glycans through their concave surface (9), whereas $NDP52_{371\text{-}381}$ bound to the opposite, convex site of $Gal8_{C\text{-}CRD}$ with a Kd of 5.2 μM, and this interaction involved an area of 496 $Å^2$ (Fig. 1A-C, fig. S1, S2). A turn formed by Leu^{374}-Ala-Tyr-Gly^{377} forces $NDP52_{371\text{-}381}$ into a hook-like structure, the C-terminus of which is further stabilized by an intramolecular hydrogen bond formed between the main chain amino group of Tyr^{380} and the side chain of Asn^{378} (Fig. 1D). Mutation of Asn^{378} in $NDP52_{368\text{-}381}$ (N378A) to prevent formation of this hydrogen bound resulted in a mutant lacking all detectable affinity for $Gal8_{C\text{-}CRD}$ (Fig. 1E, table S1). The hook-like structure of $NDP52_{371\text{-}381}$ strategically positioned its side chains in contact with several hydrophobic areas of $Gal8_{C\text{-}CRD}$: (i) NDP52 Pro^{372} contacted the indole ring of Gal8 Trp^{359}, (ii) NDP52 Tyr^{376} engaged the side chains of Gal8 Tyr^{308} and Gal8 Asn^{325}, (iii) NDP52 Leu^{374} inserted into a ridge formed by the Val^{244}, Ile^{312}, and Trp^{359} residues in Gal8, and (iv) the Pro^{379} and Tyr^{380} residues of NDP52 occupied a depression with hydrophobic walls formed by the Ile^{312}, Tyr^{314}, Lys^{321}, and Ala^{323} of Gal8 (Fig. 1B, F). The importance of these hydrophobic interactions for the binding of $NDP52_{368\text{-}381}$ to $Gal8_{C\text{-}CRD}$ was confirmed by mutational analysis (Fig. 1E, table S1). $NDP52_{368\text{-}381}$ with any of the mutations L374A, Y376A, or Y380A had severely reduced affinities for $Gal8_{C\text{-}CRD}$, as did $Gal8_{C\text{-}CRD}$ with mutations I312A, K321A, A323Y, or N325A for $NDP52_{368\text{-}381}$. $Gal8_{C\text{-}CRD}$ Y314A and W359A bound $NDP52_{368\text{-}381}$ with 7- and 5-fold

reduced affinity compared to that of the wild-type $Gal8_{C\text{-}CRD}$, respectively; whereas $Gal8_{C\text{-}CRD}$ V244A and K246A had no discernable change in binding affinity. Besides promoting hydrophobic contacts, the depression in Gal8 occupied by NDP52 Tyr^{380} also enabled the formation of hydrogen bonds between NDP52 Tyr^{380} and the side chain of Gal8 His^{328}, as well as main chain atoms of Val^{322} and Ala^{323} in Gal8 (Fig. 1D, F). Confirming the importance of these hydrogen bonds, the affinity of $NDP52_{368\text{-}381}$ Y380F and $Gal8_{C\text{-}CRD}$ H328A for wild-type $Gal8_{C\text{-}CRD}$ or $NDP52_{368\text{-}381}$, respectively, was reduced 16- and 8-fold (Fig. 1E, Tab. S1). Furthermore, hydrogen bonds were formed between the main chain atoms of the Pro^{372}-Gly^{373} and Ala^{375}-Tyr^{376} residues in NDP52 and the side chains of the Lys^{246} and Glu^{310} residues in $Gal8_{C\text{-}CRD}$, respectively (Fig. 1D, F). Mutational analysis of $Gal8_{C\text{-}CRD}$ revealed that Glu^{310}, but not Lys^{246}, was essential for binding to $NDP52_{368\text{-}381}$ (Fig. 1E, Tab. S1). Altogether, $NDP52_{371\text{-}381}$ adopted a hook-like conformation when bound to the convex surface of $Gal8_{C\text{-}CRD}$, an interaction driven by hydrophobic contacts and supported by hydrogen bonds (Fig. 1F).

Recruitment of NDP52 to galectin-8 upon *Salmonella* infection

To test whether the binding site identified for $NDP52_{368\text{-}381}$ in $Gal8_{C\text{-}CRD}$ also governs the interaction of the full-length proteins, we examined the importance of key mutations in galectin-8 by LUMIER assay. We found that galectin-8 harboring the amino acid mutations I312A or A323Y, in contrast to wild-type galectin-8, did not bind full-length NDP52 (Fig. 2A, fig. S3). To investigate the importance of the NDP52 binding site in galectin-8 in vivo, we analyzed the ability of cells to recruit NDP52 through galectin-8 to damaged vesicles containing *S.* Typhimurium as an essential step in inducing autophagy in response to bacterial infection. Consistent with our previous report (8), depletion of galectin-8 in HeLa cells abrogated NDP52 recruitment to damaged vesicles containing *S.* Typhimurium (Fig. 2B). Expression of siRNA-resistant wild-type galectin-8 restored this activity. In contrast, NDP52 recruitment was not restored in cells transfected with siRNA-resistant mutant galectin-8, Gal8 I312A or A323Y (Fig. 2B), even though both mutant proteins were fully functional in detecting *S.* Typhimurium--induced membrane damage (Fig. 2C, D). We conclude that the binding site in galectin-8 identified in our structure is essential for the recruitment of the autophagy receptor NDP52 to cytosol-exposed *S.* Typhimurium.

Sterical hindrance between NDP52 and most nonbinding galectin CRDs

Having characterized the binding site for NDP52 in $Gal8_{C\text{-}CRD}$, we investigated the features that prevent other human galectins from binding NDP52. A multiple sequence alignment of CRDs from human galectins revealed that amongst the amino acids essential for NDP52 binding, Ala^{323} is conserved in only five CRDs, including $Gal8_{C\text{-}CRD}$ (Fig. 3A). Inspection of the $Gal8_{C\text{-}CRD}$–$NDP52_{371\text{-}381}$ structure suggested that residues larger than Ala would interfere with binding (Fig. 3B). Indeed, replacing residue 323 with amino acids occurring in other galectins, such as Tyr, Phe, Met, or Val, abrogated binding of $NDP52_{368\text{-}381}$ (Fig. 3C, table S1). Ala^{323} is therefore a key specificity determinant and most galectin CRDs do not bind NDP52 because of sterical hindrance in this position or, as is the case in the $Gal12_{N\text{-}CRD}$ mimetic $Gal8_{C\text{-}CRD}$ A323S, because hydrophobic contacts to $NDP52^{P379}$ are disfavoured. In the four human galectin CRDs that harbor Ala^{323} but do not bind NDP52, the neighboring residue Ile^{312} is not conserved (Fig. 3A). Because Ile^{312} is a major contributor to the same hydrophobic pocket, we tested the impact of naturally occurring Ile^{312} replacements on NDP52 binding. $Gal8_{C\text{-}CRD}$ I312Q or I312W, which mimic the residues found in Gal3 or in the C-CRD of Gal9, respectively, did not bind $NDP52_{368\text{-}381}$ (Fig. 3C, Tab. S1). In contrast, $Gal8_{C\text{-}CRD}$ variants carrying certain aliphatic residues in this position, such as I312L or I312V, which mimic the C-CRD of Gal12 or the N-CRD of Gal8, respectively, retained nearly wild-type affinity for $NDP52_{368\text{-}381}$. Altogether, the lack of conservation of just two residues in galectin-8, the adjacently located Ile^{314} and Ala^{323},

sufficed to explain the lack of NDP52 binding in all human galectin CRDs except the C-CRD of Gal12 and the N-CRD of Gal8. For these CRDs, the contribution of two aromatic residues, Tyr^{314} and Trp^{359}, was investigated further because their individual replacement moderately decreased affinity for NDP52 (Fig. 1E, table S1). Indeed, $Gal8_{C\text{-}CRD}$ Y314L/H328G/W359Δ and $Gal8_{C\text{-}CRD}$ Y314M/K321Q/W359S, mimicking the C-CRD of Gal12 and the N-CRD of Gal8, respectively, showed no detectable binding to $NDP52_{368\text{-}381}$ (Fig. 3C, table S1). Therefore, the data indicated that selectivity of NDP52 for $Gal8_{C\text{-}CRD}$ is primarily caused by sterical hindrance in the CRDs of other galectins that do not bind; whereas the lack of conserved contact residues in nonbinding CRDs contributed relatively less to this selectivity.

Discussion

This study showed how information about defects in the integrity of vesicular membranes, revealed by the exposure of glycans otherwise hidden inside the vesicular lumen, is transduced with high selectivity from galectin-8 to NDP52. A crystal structure of galectin-8 bound to NDP52 revealed how the two proteins engage selectively. Binding of NDP52 to galectin-8 occurs through a hook-like structure in NDP52 that positions multiple side chains for mainly hydrophobic contacts with galectin-8. In contrast, binding of NDP52 to most other galectins is prevented by simple sterical hindrance. The key residue for the selective interaction with NDP52 is $Gal8_{C\text{-}CRD}$ Ala^{323}, located at the bottom of a hydrophobic binding pocket, due to its low degree of conservation amongst galectin CRDs and an absolute requirement for a very small hydrophobic side chain in this position.

Inducing selective autophagy in response to vesicle damage removes potentially harmful membrane remnants from the cytosol (8, 11, 16). In addition, the ability of galectin-8 and NDP52 to detect and engulf pathogen-damaged vesicles bestows cells with a mechanism to deliver vesicle-damaging pathogens, such as *S.* Typhimurium, to autophagosomes for subsequent destruction (8). This pathway may impose a significant hurdle to professional cytosol-dwelling bacteria as their life style demands vacuolar damage during their translocation into the host cytosol. Galectin-mediated detection of membrane damage following bacterial infection also triggers inflammatory signaling, although the proteins involved and details of their interaction remain to be established (17). It will be interesting to determine which galectin(s) link vesicle damage to inflammatory signalling and whether advantage has been taken by pathogens, or could be taken therapeutically, to differentially manipulate individual pathways. The structure of galectin-8 bound to NDP52 provides the basis for experimental attempts to selectively manipulate galectin-8 signaling to autophagy.

Material and Methods

Antibodies

The antiserum against NDP52 used for immunofluorescence was a kind gift from John Kendrick-Jones (MRC LMB, Cambridge). Antibody detecting the Flag tag was purchased from Sigma.

Plasmids

M5P or closely related plasmids were used to produce recombinant MLV for the expression of galectin-8 in mammalian cells (18)..

Cell culture and infection with bacteria

HeLa cells, obtained from the European Collection of Cell Cultures, were grown in Iscove's Modified Dulbecco's Media (IMDM) supplemented with 10% FCS at 37°C in 5% CO_2. *S.*

Typhimurium (strain 12023), kindly provided by David Holden (Imperial College, London), was grown overnight in LB and sub-cultured (at a ratio of 1:33) in fresh LB for 3.5 hours prior to infection. HeLa cells in 24-well plates were infected with 20 μl of such cultures for 15 min. Following two washes with warm phosphate buffered saline (PBS, pH 7.4) cells were cultured for 45 min in IMDM containing 100 μg/ml gentamycin.

RNAi

5×10^4 cells per well were seeded in 24-well plates. The following day cells were transfected with 40 pmol of siRNA against galectin-8 (siGal8#38; Invitrogen) using Lipofectamine 2000 (Invitrogen) in Optimem medium (Invitrogen). Optimem was replaced with complete IMDM medium after 4 hours and experiments were performed after 72 hours. siGal8#38 and galectin-8 resistant to siGal8#38 have been described previously (8).

LUMIER assay

The LUMIER assay was performed as previously described (19,20)**.** Binding assays with pairs of putative interactors, one fused to luciferase and the other fused to Flag, were performed in LUMIER lysis buffer [150 mM NaCl, 0.1% (v/v) Triton-X100, 20 mM Tris–HCl (pH 7.4), 5% (v/v) glycerol, 5 mM EDTA and **Complete**™ Protease Inhibitor Cocktail (Roche)]. After washing in lysis buffer, proteins were eluted with Flag-peptide in Renilla lysis buffer (Promega). Relative luciferase activity represents the ratio of activity eluted from beads to that from lysates.

Microscopy

HeLa cells were grown on glass cover slips prior to infection. Following infection, cells were washed twice with warm PBS and fixed in 4% paraformaldehyde in PBS for 30 min. Cells were washed twice in PBS and quenched with PBS (pH 7.4) containing 1 M glycine before being blocked and permeabilized for 1 hour in PBS containing 0.1% (w/v) saponin and 2% (w/v) BSA. Cover slips were incubated with antibody against NDP52 (1:500 in PBS containing 0.1% (w/v) saponin and 2% (w/v) BSA), followed with Alexa488-conjugated secondary antibody for 1 hour and mounted in medium containing DAPI (Vector Laboratories). Confocal images were captured with a −63X, 1.4 numerical aperture objective on a Zeiss 780 microscope.

Protein expression and purification

The open reading frame of the C-terminal CRD domain of human galectin-8 (residues 228-359) was amplified from a human brain cDNA library (Clontech) and inserted into a modified pET-28a(+) expression vector (Novagen). The modified pET-28a (+) plasmid contained an N-terminal 6×His tag, and a tobacco etch virus (TEV) protease cleavage site. Mutants were generated by site-directed mutagenesis and confirmed by sequencing. Proteins were expressed in *Escherichia coli* strain BL21(DE3) upon induction with 1 mM isopropyl-β-D-1-thiogalactopyranoside (IPTG) overnight at 16°C. Bacterial pellets were resuspended in buffer A (20 mM Tris-HCl, 500 mM NaCl, pH 8.0) and lysed by sonication on ice. Soluble proteins were purified using a Ni^{2+}-chelating column (GE Healthcare), followed by gel-filtration (Hiload 16/60 Superdex 75 column, GE Healthcare). For crystallization trials, the purified protein was concentrated to approximately 10 mg ml^{-1} in buffer B (20 mM Tris-HCl, 200 mM NaCl, 1 mM EDTA , pH 7.0).

Peptide synthesis

Peptides were synthesized by GL Biochem (Shanghai), and purified by reverse-phase HPLC. Stock solutions (5-15 mM) were prepared in buffer B.

Isothermal titration calorimetry (ITC)

Proteins and peptides were dialyzed against buffer B, and adjusted to 0.13 mM and 1.3 mM, respectively. ITC experiments were carried out in a MicroCal iTC200 instrument (GE healthcare) at 25°C and analyzed using ITC data analysis module of Origin 7.5 (OriginLab Corporation) provided with the iTC200 calorimeter.

Crystallization, data collection, and structure determination

$Gal8_{C\text{-}CRD}$ and $NDP52_{368\text{-}381}$, mixed at a 1:2 molar ratio, were crystallized in 2% PEG 400, 0.1 M HEPES sodium pH 7.5, 2.0 M ammonium sulfate, at 10°C. Crystals were soaked in cryoprotectant made of mother liquor supplemented with 25% glycerol, before being flash frozen in liquid nitrogen. Data sets were collected on beam line 17U at Shanghai Synchrotron Radiation Facility (SSRF). The structure of the $NDP52_{368\text{-}381}$-$hGal8_{C\text{-}CRD}$ complex was solved by molecular replacement using the program MOLREP (21), employing the free $hGal8_{C\text{-}CRD}$ (PDB coordinate 4FQZ) as the search model. The $NDP52_{368\text{-}381}$ peptide was then modeled in COOT (22)and the structure of $NDP52_{368\text{-}381}$-$hGal8_{C\text{-}CRD}$ domain was refined using PHENIX.refine (23). Crystal diffraction data and refinement statistics are displayed in Table S1. Structure analysis was performed by using COOT and PyMOL (http://www.pymol.org/).

Supplementary Material

Refer to Web version on PubMed Central for supplementary material.

Acknowledgments

We thank John Kendrick-Jones for the NDP52 antiserum, David Holden for *S.* Typhimurium 12023, Dr. Hongda Huang, Dr. Weiwei Wang and Juncheng Wang for helpful discussions, Dr. Jianye Zang, Minhao Wu, Zhenhua Shao, Yang Zou and Debiao Zhao for assistance with X-ray data collection and data processing, Dr. Congzhao Zhou and Wang Cheng for assistance in ITC experiments, and the staff at BL17U of Shanghai Synchrotron Radiation Facilities (SSRF) for assistance with X-ray data collection. **Funding:** Work in the group of YS is supported by the National Basic Research Program of China (973 Program, grants 2011CB966302, 2012CB917201 and 2011CB911104) and the Chinese National Natural Science Foundation (grant 30830031, 31170693). Work in the group of F.R. is supported by the Medical Research Council (U105170648) and The National Association for Colitis and Crohn's Disease (M/11/3).

References

1. Mizushima N, Yoshimori T, Ohsumi Y. The role of atg proteins in autophagosome formation. Annu. Rev. Cell Dev. Biol. 2011; 27:107–132. [PubMed: 21801009]
2. Levine B, Mizushima N, Virgin HW. Autophagy in immunity and inflammation. Nature. 2011; 469:323–335. [PubMed: 21248839]
3. Randow F, Münz C. Autophagy in the regulation of pathogen replication and adaptive immunity. Trends in Immunology. 2012; 33:475–487. [PubMed: 22796170]
4. Johansen T, Lamark T. Selective autophagy mediated by autophagic adapter proteins. Autophagy. 2011; 7:279–296. [PubMed: 21189453]
5. Thurston TLM, Ryzhakov G, Bloor S, von Muhlinen N, Randow F. The TBK1 adaptor and autophagy receptor NDP52 restricts the proliferation of ubiquitin-coated bacteria. Nat Immunol. 2009; 10:1215–1221. [PubMed: 19820708]
6. Zheng YT, et al. The adaptor protein p62/SQSTM1 targets invading bacteria to the autophagy pathway. J Immunol. 2009; 183:5909–5916. [PubMed: 19812211]
7. Wild P, et al. Phosphorylation of the Autophagy Receptor Optineurin Restricts Salmonella Growth. Science. 2011; 333:228–233. [PubMed: 21617041]

8. Thurston TLM, Wandel MP, von Muhlinen N, Foeglein A, Randow F. Galectin 8 targets damaged vesicles for autophagy to defend cells against bacterial invasion. Nature. 2012; 482:414–418. [PubMed: 22246324]
9. Houzelstein D, et al. Phylogenetic analysis of the vertebrate galectin family. Mol Biol Evol. 2004; 21:1177–1187. [PubMed: 14963092]
10. Rabinovich GA, Toscano MA. Turning "sweet" on immunity: galectin–glycan interactions in immune tolerance and inflammation. Nat. Rev. Immunol. 2009; 9:338–352. [PubMed: 19365409]
11. Paz I, et al. Galectin-3, a marker for vacuole lysis by invasive pathogens. Cell Microbiol. 2009; 12:530–544. [PubMed: 19951367]
12. von Muhlinen N. LC3C, bound selectively by a non-canonical LIR motif in NDP52, is required for anti-bacterial autophagy. Mol Cell. 2012:1–56. in press.
13. Nagae M, et al. Crystal structure of the galectin-9 N-terminal carbohydrate recognition domain from Mus musculus reveals the basic mechanism of carbohydrate recognition. J Biol Chem. 2006; 281:35884–35893. [PubMed: 16990264]
14. Seetharaman J. X-ray Crystal Structure of the Human Galectin-3 Carbohydrate Recognition Domain at 2.1-A Resolution. Journal of Biological Chemistry. 1998; 273:13047–13052. [PubMed: 9582341]
15. Bourne Y, et al. Crosslinking of mammalian lectin (galectin-1) by complex biantennary saccharides. Nat Struct Biol. 1994; 1:863–870. [PubMed: 7773775]
16. Dupont N, Temime Smaali N, Lafont F. How ubiquitination and autophagy participate in the regulation of the cell response to bacterial infection. Biol. Cell. 2010; 102:621–634. [PubMed: 21077843]
17. Dupont N, et al. Shigella Phagocytic Vacuolar Membrane Remnants Participate in the Cellular Response to Pathogen Invasion and Are Regulated by Autophagy. Cell Host and Microbe. 2009; 6:137–149. [PubMed: 19683680]
18. Randow F, Sale JE. Retroviral transduction of DT40. Subcell Biochem. 2006; 40:383–6. [PubMed: 17623925]
19. Barrios-Rodiles M, et al. High-throughput mapping of a dynamic signaling network in mammalian cells. Science. 2005; 307:1621–5. [PubMed: 15761153]
20. Ryzhakov G, Randow F. SINTBAD, a novel component of innate antiviral immunity, shares a TBK1-binding domain with NAP1 and TANK. EMBO J. 2007; 26:3180–90. [PubMed: 17568778]
21. Vagin A, Teplyakov A. Molecular replacement with MOLREP. Acta Crystallogr D Biol Crystallogr. 2010; 66:22–5. [PubMed: 20057045]
22. Emsley P, Lohkamp B, Scott WG, Cowtan K. Features and development of Coot. Acta Crystallogr D Biol Crystallogr. 2010; 66:486–501. [PubMed: 20383002]
23. Adams PD, et al. PHENIX: a comprehensive Python-based system for macromolecular structure solution. Acta Crystallogr D Biol Crystallogr. 2010; 66:213–21. [PubMed: 20124702]

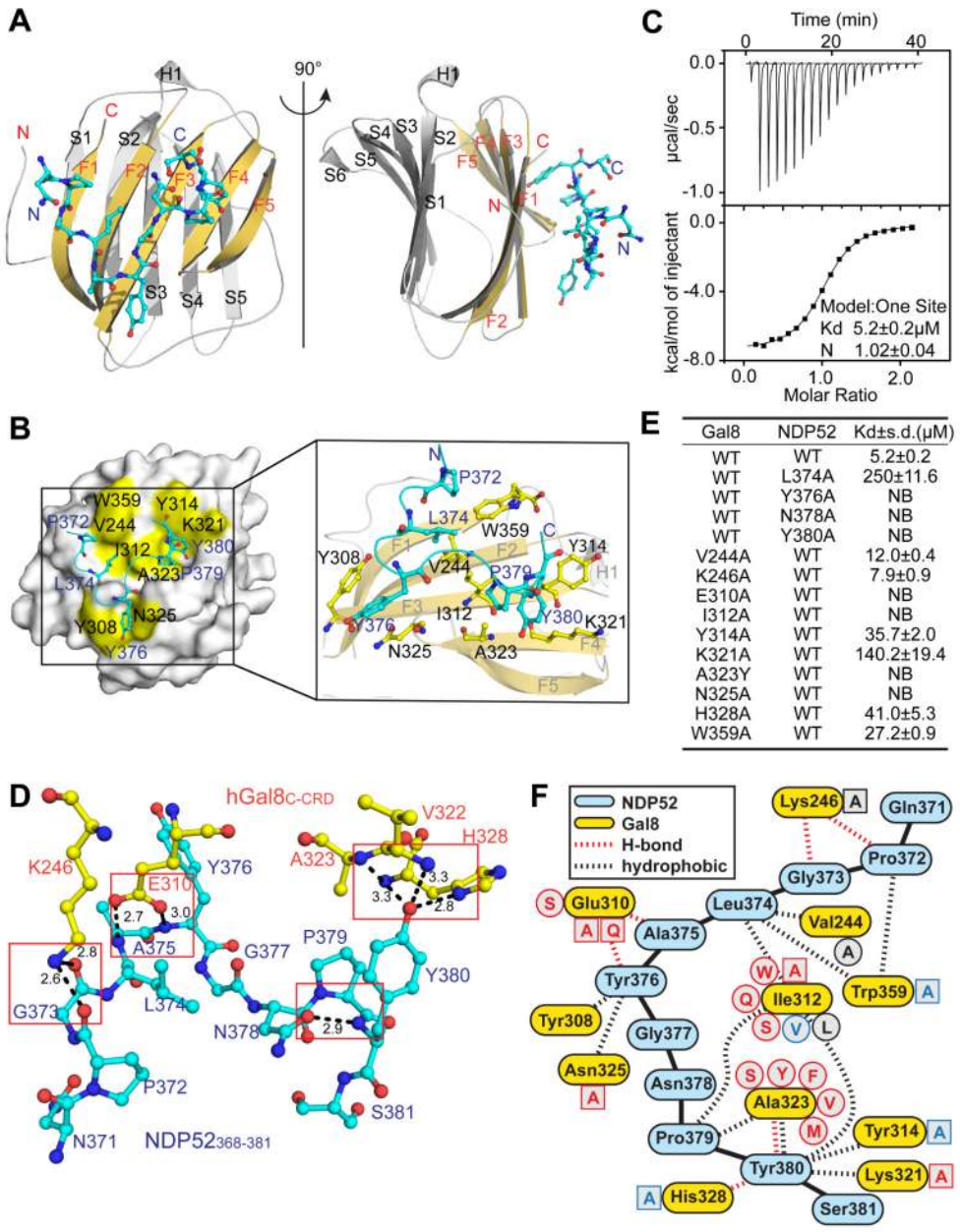

Gal8	NDP52	Kd±s.d.(μM)
WT	WT	5.2±0.2
WT	L374A	250±11.6
WT	Y376A	NB
WT	N378A	NB
WT	Y380A	NB
V244A	WT	12.0±0.4
K246A	WT	7.9±0.9
E310A	WT	NB
I312A	WT	NB
Y314A	WT	35.7±2.0
K321A	WT	140.2±19.4
A323Y	WT	NB
N325A	WT	NB
H328A	WT	41.0±5.3
W359A	WT	27.2±0.9

Figure 1. The molecular basis of the interaction between $Gal8_{C\text{-}CRD}$ and $NDP52_{368\text{-}381}$

(A) Cartoon representation of $Gal8_{C\text{-}CRD}$ (yellow and grey) in complex with $NDP52_{368\text{-}381}$ (cyan). F1-F5, S1-S6 numbering of β-strands. **(B)** Hydrophobic contacts between $Gal8_{C\text{-}CRD}$ and $NDP52_{368\text{-}381}$. Residues of $Gal8_{C\text{-}CRD}$ involved in hydrophobic interaction are colored yellow and labeled in black. NDP52 in cyan. **(C)** ITC data for the interaction of $NDP52_{368\text{-}381}$and $Gal8_{C\text{-}CRD}$ at the indicated peptide versus protein molar ratios. Top, raw data; bottom, integrated heat data. Kd, dissociation constant; N, reaction stoichiometry. **(D)** Hydrogen bonds between $Gal8_{C\text{-}CRD}$ (yellow) and $NDP52_{368\text{-}381}$ (cyan) with distances measured in Ångströms (Å). **(E)** Dissociation constants for the indicated interactions obtained through ITC. . NB: binding not detectable. **(F)** Scheme of interactions between NDP52 (blue) and galectin-8 (yellow). Single letter abbreviations indicate mutations tested in this study with colors indicating affinity (red: Kd >120 μM, blue: 27< Kd <41 μM, black:

Kd <12 μM). Circled residues occur in human galectin CRDs, squared residues are experimental mutations.

Europe PMC Funders Author Manuscripts

Europe PMC Funders Author Manuscripts

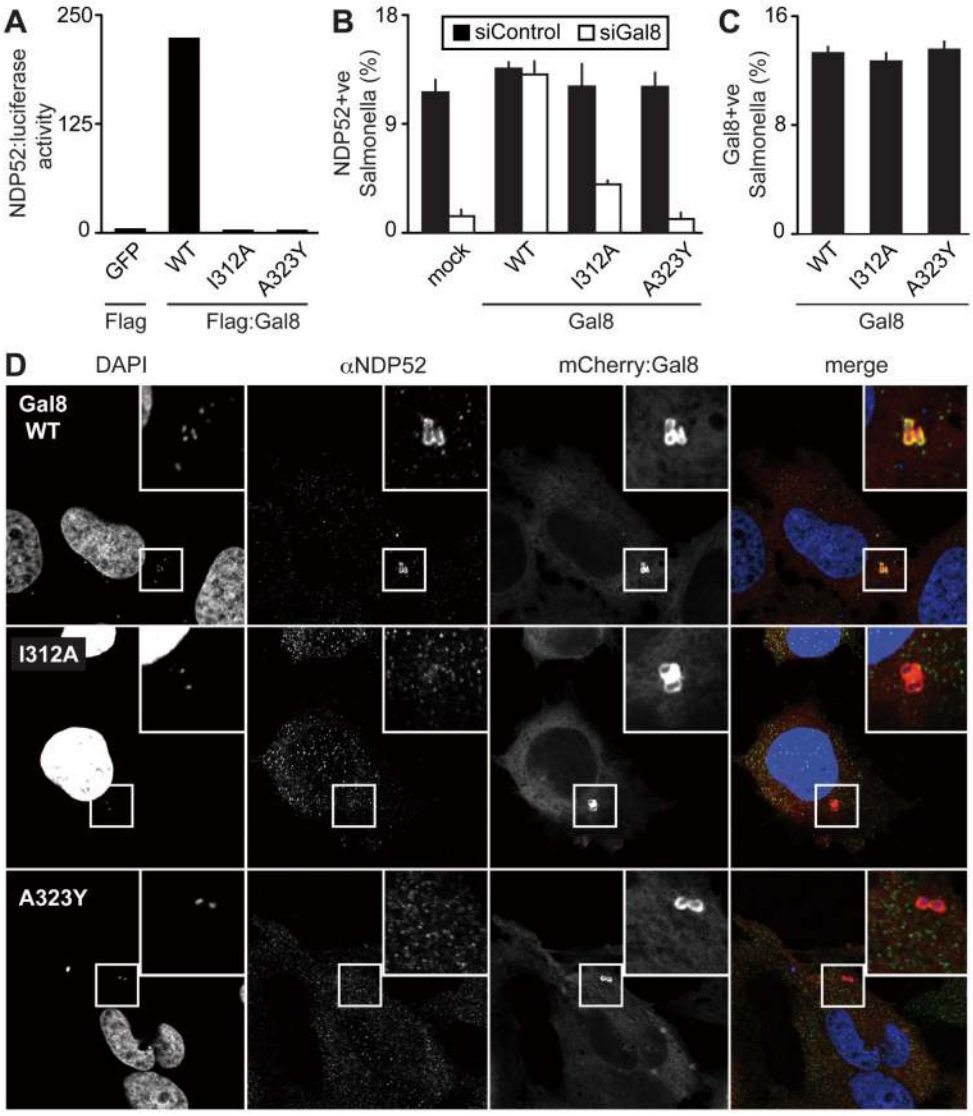

Figure 2. Functional importance of the NDP52 binding site in galectin-8 for anti-bacterial autophagy

(A) LUMIER binding assay. Normalized ratio of luciferase activity bound to anti-Flag beads to luciferase activity in lysates from 293ET cells co-expressing NDP52 fused to luciferase and the indicated Flag-tagged wild-type (WT) or mutated (I312A, A323Y) galectin-8 proteins. (**B-C**) Percentage of *S.* Typhimurium exhibiting NDP52 (**B**) or galectin-8 (**C**) recruitment at 1 hour post-infection in Hela cells expressing the indicated siRNA-resistant WT or mutated galectin-8 alleles fused to mCherry as determined by fluorescence microscopy. Cells were treated with control siRNA (siControl) or siRNA against galectin-8 (siGal8) **(B)** or only siGal8 **(C).**. Mean and s.d. were quantified from quadruplicate cultures (n>200 bacteria per coverslip), and representative confocal images from siGal8-treated cells are shown (**D**).

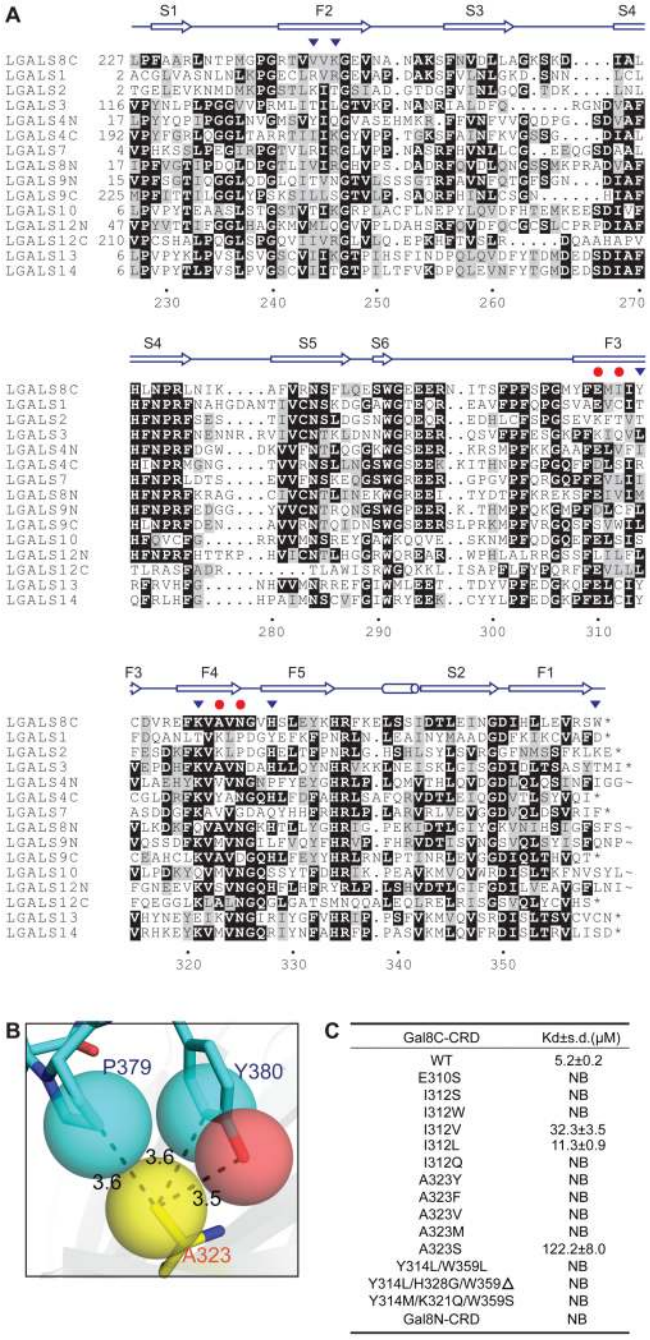

Gal8C-CRD	Kd±s.d.(μM)
WT	5.2±0.2
E310S	NB
I312S	NB
I312W	NB
I312V	32.3±3.5
I312L	11.3±0.9
I312Q	NB
A323Y	NB
A323F	NB
A323V	NB
A323M	NB
A323S	122.2±8.0
Y314L/W359L	NB
Y314L/H328G/W359Δ	NB
Y314M/K321Q/W359S	NB
Gal8N-CRD	NB

Figure 3. The molecular basis for the specificity of NDP52 for galectin-8

(A) For galectins containing two CRDs, N- and C-terminal domains are indicated. Red dots and black triangles indicate residues in $Gal8_{C\text{-}CRD}$ that, if mutated, prevented or impaired binding to $NDP52_{368\text{-}381}$, respectively.

(B) Close-up view of Gal8 Ala^{323} (yellow) in contact with the γ-carbon of the NDP52 Pro^{379} and the ε-carbon and hydroxyl oxygen of the NDP52 Tyr^{380} side chain (blue and red). Van der Waals volumes of key atoms rendered as transparent spheres.

(C) Dissociation constants for the interaction of $NDP52_{368\text{-}381}$ with the indicated $Gal8_{C\text{-}CRD}$ variants obtained ITC. NB: binding not detectable.

Table 1
Summary of diffraction data and structure refinement statistics

	Galectin-8$_{C\text{-}CRD}$-NDP52$_{368\text{-}381}$
Data collection	
Space group	C222
Cell dimensions	
a, b, c (Å)	76.087 124.826 43.737
α, β, γ (°)	90.00 90.00 90.00
Resolution(Å)	50-2.02(2.05-2.02)[a]
R_{merge}(%)	8.5(33.3)
I/σI	20.34(6.79)
Completeness (%)	99.9(100)
Redundancy	5.3(4.8)
Refinement	
No. reflections (overall)	13992
No. reflections (test set)	701
R_{work}/R_{free}(%)	17.67/21.61
No. non-H atoms	
Gal8$_{C\text{-}CRD}$	1162
NDP52	81
Glycerol	12
Water	119
B-factors	
Gal8$_{C\text{-}CRD}$	21.59
NDP52	27.15
Glycerol	20.45
Water	32.18
R. m. s. deviations	
Bond lengths (Å)	0.008
Bond angles (°)	1.257

[a]Values in parentheses are for highest-resolution shell.